Materials Science Forum
ISSN: 1662-9752, Vol. 1020, pp 41-48
doi:10.4028/www.scientific.net/MSF.1020.41

Submitted: 2020-06-18
Accepted: 2020-07-24
Online: 2021-02-01

Investigation Toiler Weld Blank of SSM 2024 Aluminum Alloys by Friction Stir Welding Joint

Yongyuth Dunyakul[1,a*], Chaiyoot Meengam[2,b*] and Dech Maunkhaw[3,c]

[1,3]Department of Industrial Engineering, Faculty of Engineering, Rajamangala University of Technology Srivijaya, Songkhla, Thailand

[2,4]Faculty of Industrial Technology, Songkhla Rajabhat University, Songkhla, Thailand
[a]Dyongyuth@gmail.com*, [b]Chaiyoot.me@skru.ac.th*, [c]Dechmaunkhaw@yahoo.com

Keywords: Toiler Weld Blank; SSM 2024 Aluminium Alloy; Friction Stir Welding.

Abstract. The objective of this research was to investigate variables that affected the adhesion of the welded joints for TWBs with FSW in the SSM 2024 aluminum alloys. The results clearly showed that there was a good adhesion of the samples in every experiment. Longitudinal voids can also been found on the top surface of some variables. The average size of cross-links structure of Al_2Cu phase (β phase) in SZ, broken into smaller pieces, was around 4 to 7 μm and evenly mixed with alpha phase (α phase). The effect of fracture of Al_2Cu phase promoting better mechanical properties. The appropriate tensile strength from the experiment came from variables at the work angle at 15°, rotation speed at 2720 rpm, and welding speed 60 mm/min which provided maximum tensile strength value at 205.0 MPa and the maximum average hardness at 132.4 HV, higher than the weld region. The assessment results showed that the differences in welding variables resulted in different mechanical properties.

Introduction

The Tailored Welded Blanks (TWBs) is the principle of welding samples with different thickness, used in the automotive industry [1], in order to reduce the weight of various parts of the car to be lighter. The conceptual model TWBs due to its low cost can reduce energy consumption and can also reduce the use of materials in a process. This means a thick material will be chosen in a case that requires high load; on the contrary, a material with less thickness will be used in an area that does not need high load. This leads to the selection of materials with suitable mechanical properties for each piece with good engineering design principles. However, welding of different thickness materials is not easy due to the different material thickness resulting in difficulty to control welding parameters. Especially, the appropriate variables in TWBs with friction stir welding method (FSW) have not been well studied yet. The FSW was invented by The Welding Institute in 1991 [2] and several methods have been developed to be suitable for use in other industries, now extensively used in the automotive industry such as door panels, driveshafts, and space frames [3]. The advantages of FSW are as follows: low distortion and shrinkage after welds, excellent mechanical properties, energy saving, no filler wire required, no gas shielding, can do long weld, and environmentally friendly [4]. However, welding parameters relating to the heat generated during the welding process significantly affect the adhesion of the samples, and studying these variables that affect the welding of different thickness of materials is therefore a challenge and interesting. Popular materials with FSW were light metals such as aluminum alloy, magnesium, titanium, and copper. The aluminum alloy is extensively used in the automotive industry to manufacture automotive parts. The Semi-Solid Metal 2024 aluminum alloys (SSM) [5] developed from the molding by releasing gas bubbles are also used to produce automotive parts. The TWBs of SSM 2024 aluminum alloys with FSW so is interesting. Since, this idea could support the automotive manufacturing parts industry or welding to repair damaged samples after used. The main purpose of this research is to investigate parameters affecting TWBs of SSM 2024 aluminum alloys with FSW. The result analysis focuses on the tensile strength and the changes of microstructure at the joint, and the appropriate variables from the experiment will be evaluated. The results of microstructure analysis in stir zone and affected thermal-mechanical zone will be presented with the analysis of base materials after welding joints by using a scanning electron microscopy.

Experimental Procedures

SSM 2024 aluminum alloys, containing copper, manganese, and magnesium, were used in the experiment. The microstructure of the alpha phase (α) was a globular shape and the beta phase (β) had a shape of cross-links formed Al_2Cu phase, which was inserted between the grain boundaries. The chemical composition and mechanical properties are shown in Table 1. The SSM 2024 aluminum alloys were produced from gas induces semi-solid methods (GISS). The GISS technique is an aluminum casting process, a semi-solid state with cast temperature 640 °C, which releases gas bubbles through the porous graphite rod at a pressure of 8 liters per minute. Then, it is compressed at 250 bars and cooled. In this experiment, the two rectangular shape samples were prepared with two different thickness of dimension 50x100x3 mm and 50x100x6 mm, respectively.

Table 1 Chemical composition and properties of SSM 2024 aluminum alloy [6]

Materials	Cu	Fe	Mg	Mn	Si	Ti	Zn	Al
2024	3.8-4.9	0.5	1.2-1.8	0.3-0.9	0.5	0.15	0.25	Bal.
Ultimate tensile strength (MPa)			**Elongation (mm)**			**Hardness Vickers**		
185			20			114		

The variables in the experiment obtained from preliminary studies are rotation speed as 1110, 1750 and 2720 rpm, welding speed as 30, 60 and 90 mm/min, and 2 levels of tilt work angle as 10 and 15 degrees shown in Table 2. For TWBs of FSW, tools made from SKD 61 (JIS Stranded) were used. The size of the tool was a 20 mm shoulder, a 4 mm tool pin, and 3.2 mm in length. For FSW, the samples should be camped with a butt joint. Then, samples were jointed in different thickness according to the theory of TWBs, with the 6 mm thickness samples were on the advancing side (AS) and the 3 mm thickness samples were on the retreating side (RS). The tilt angle according to the sample thickness was adjusted at 10 or 15 degrees, presented in Fig.1(a). After that, the travel angle for welding was adjusted at 3 degrees, presented in Fig.1(b). The direction of the welding rotation was clockwise. The tool was pressed on the welding position at a constant speed of 3.9 mm per minute until the shoulder of the tool contact with the surface of the sample. Therefore, the pressure was exerted on the samples with the depth of the plug at 0.8 mm. During this period, although the friction behavior between the tool and the surface of the sample would be high enough to cause damage to the tool, it would generate heat as well. The resulting heat weakened the material in the stir zone, which is required to maintain a welding time of 20 sec. Then, the welding machine was controlled in the specified direction, following by maintaining welding time before pulling the tool up by another 20 sec, to complete the keyhole form in stir zone after welding. The different variables used TWBs with FSW in the SSM 2024 aluminum alloys are shown in Table 2.

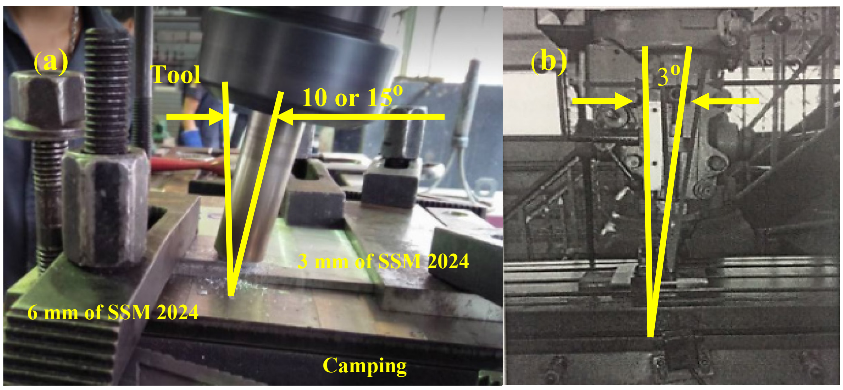

Figure 1. Shows photos TWBs with FSW of SSM 2024 aluminum alloy.

Table 2 The variables used in the experiment

Welding Speed (mm/min)	Tilt work Angle (Degree)	Rotation Speed (rpm)
30	10	1110
		1750
		2720
	15	1110
		1750
		2720
60	10	1110
		1750
		2720
	15	1110
		1750
		2720
90	10	1110
		1750
		2720
	15	1110
		1750
		2720

The size and shape of the pull samples for tensile strength were prepared with the American Society of Testing and Materials according to ASTM E8 standard. The Testometric model: M500-25KN tensile strength was used to test the samples at room temperature and at a testing speed at 1.67x 10^2 mm per min. Matsuzawa model MMT-X7 for Vickers hardness methods was used to test the hardness, by using a diamond pyramid at the end of the indenter at an angle of 136 degrees, soaking time 10 seconds and apply pressure by 10 KN test (HV_{10}). The samples were measured on the cross-section at every 1.5 mm intervals away from the center of the weld zone as presented in Fig.2. Assessing the microstructure in weld zone and other areas, the microstructure was anylazed by a FEI-Quanta scanning electron microscopy model 400 from Japan. The sample preparation was carried out by grinding surfaces with P180, 360, 800, 1000 and 1200 grit SiC paper respectively. Then, polished by grinding the samples surface with alumina powder size 5, 3 and 1 µm. After that, the samples were etched with Keller's acid, and cleaning with acetone for 30 seconds. Lastly, the samples were examined changes in microstructure, defects, and particle distribution characteristics the in weld area.

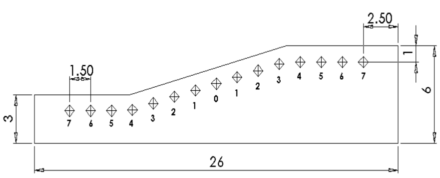

Figure 2. Schematic location of examining hardness on TWBs with FSW for SSM 2024 aluminum alloy.

Results and Discussion

The results of FSW of TWBs of samples show a good tendency of both mechanical and metallurgical properties; the samples after welding can be attached. The experimental results are presented as follows:

Microstructure Results

The top surface of the samples is presented in Fig.3, with different roughness. The heat generated during TWBs with FSW affected the appearance of the top surface, with a rotation speed of 2720 rpm. It showed the surface with high roughness comparing to other variables presented in Fig.3(c, f, i, l, o and r) respectively. Simultaneously, the high heat from friction between the shoulder tool with samples surface resulting in the formation of flash [7], affecting the integrity of the joint, and reducing defects. However, a high overheat caused the material to be softer which could potentially cause the welding tool to push material out of SZ, becoming flash defect. The longitudinal voids that parallel to the travel direction of the weld were shown due to lower heat which directly affected the difficulty of materials to flow and mix which is leading to the presence of longitudinal viods in Fig.3(h, i, and m). It can be seen that heat input is important for TWBs of FSW, and heat generation can be calculated by the given as [8]:

$$q_{\mathrm{fi}} = 2\pi\mu F n R_i n \tag{1}$$

R*i* is the distance from the calculated point to the axis of the rotating tool, n is the rotation speed and F*n* is the coefficient of the friction between the tool and samples surface. For the top surface of the samples, other variables had a complete appearance presented in Fig.3.

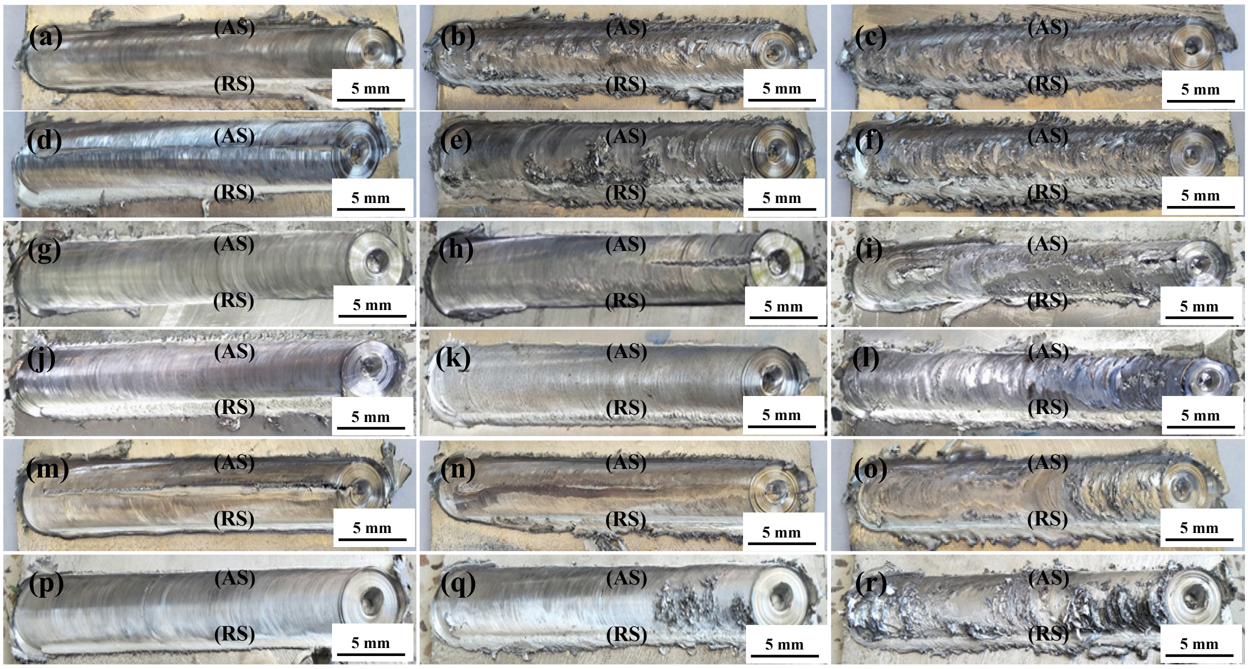

Figure 3. The top view photograph of welding surface of different variables of TWBs to FSW.

Figure 4 shows the characteristics of the Al_2Cu particle distribution at the SZ inspected by SEM, with the tilt angle at 10º, rotation speed at 1750 rpm and welding speed 30 mm/ min at a magnification of 800X. The formation of a large void at the end of the pin tool was observed resulting from low heat [9] while TWBs with FSW leading to the void is presented in Fig.4(a). At 800X magnification, it showed the distribution of Al_2Cu phase from cross-link structure, which was inserted at the grain boundary of the globular structure. It can be clearly seen that some of the Al_2Cu phase had been destroyed, broken and crushed by a friction force into small particles merged with the aluminum matrix as presented in Fig.4(d and e). The average size of Al_2Cu phase was 12 to 18 µm. At the same time, a small void was found at the SZ which was the result of variables that affected heat.

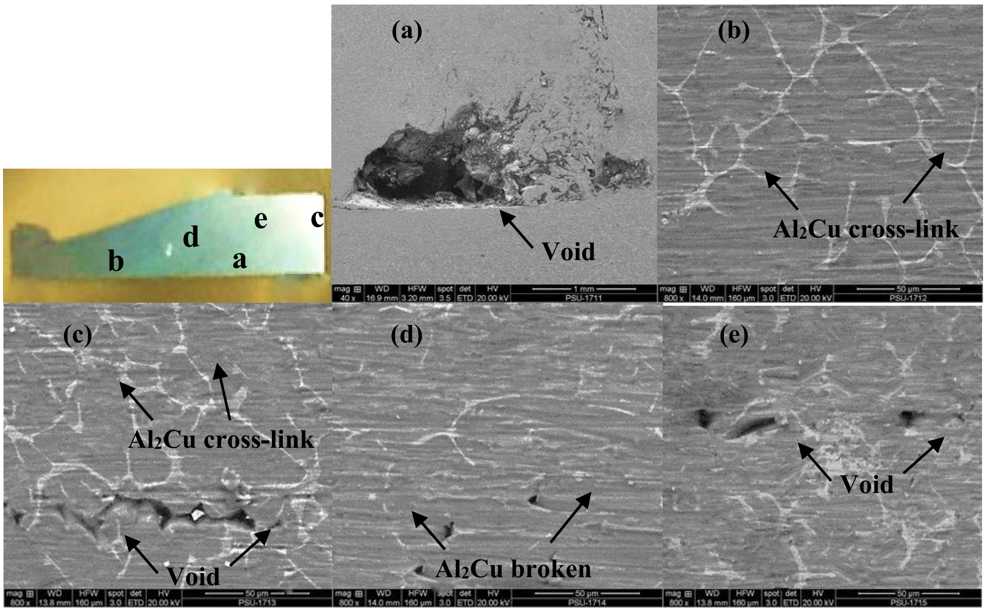

Figure 4. The photograph of TWBs with FSW for the tilt angle at 10°, rotation speed at 1750 rpm, and welding speed 30 mm/min by SEM.

TMAZ was an area that received the heat from TWBs with FSW SSM 2024 aluminum alloy; however, stress behavior was less comparing to SZ, affecting cross-link structure of Al_2Cu phase which is hard to be destroyed. The average size of Al_2Cu phase was 12 to 18 µm in TMAZ as presented in Fig.5 (c and d). On the other hand, from the structural examination in SZ with the tilt angle at 15°, rotation speed at 2720 rpm, and welding speed 60 mm/min, it was found that Al_2Cu phase changed to a smaller shape with an average size of 4 to 7 µm. Moreover, those particles had a uniform distribution leading to good hardness properties as presented in Fig.5 (a, d and e). Also, the experiment of the above variables showed that the low number of voids, which supports good mechanical properties [10]. The TMAZ region near the SZ influenced by friction froce and heat, which is the cause of Al_2Cu particle fracture, is presented in Fig.5 (b and e). The different variables of the experiment led to the difference in particle size, which could be found by examining the structure of the SZ.

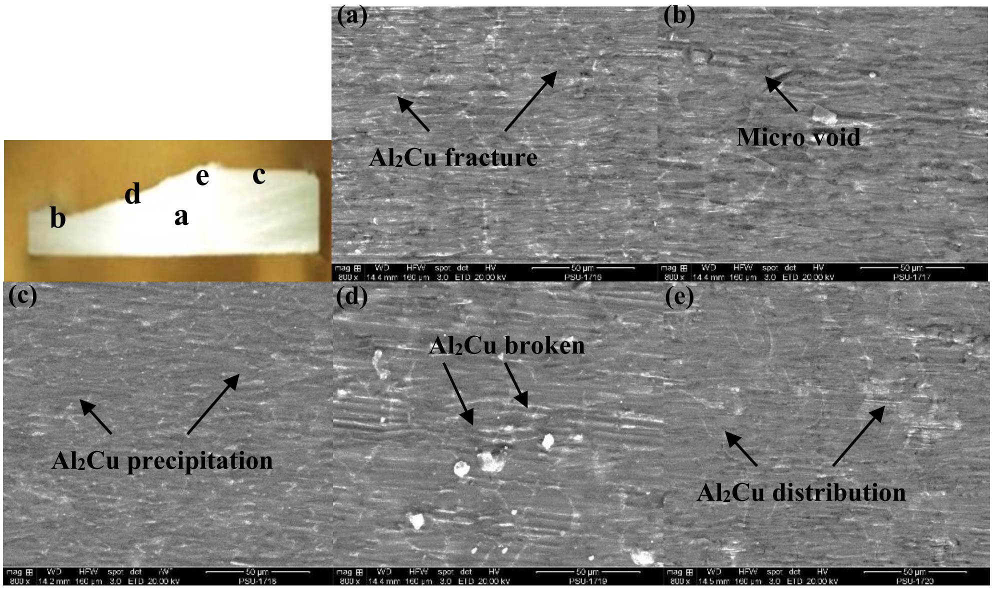

Figure 5. The photograph of TWBs with FSW for the tilt angle at 15°, rotation speed at 2720 rpm, and welding speed 60 mm/min by SEM.

Tensile Strength Results

The results show good tensile strength in all experiments. It can be seen that the variables in the experiment had different tensile strengths. To illustrate, tilt angle at 15^{o} tends to provide better tensile strength than tilt angle at 10^{o}. This is caused by the appropriate material flow. A maximum average tensile strength of 205.0 MPa at the tilt angle at 15^{o}, rotation speed at 2720 rpm, and welding speed 60 mm/min was the accepted optimum condition. The tilt angle of TWBs with FSW had a clear effect on the changes in tensile strength. As seen from the above observations, the increased tensile strength and tilt angle also show defects. The tilt angle at 10^{o}, rotation speed at 1750 rpm, and welding speed 60 mm/min had a minimum average tensile strength of 71.3 MPa and caused longitudinal voids. However, when the welding speed was increased from 60 to 90 mm/min, tensile strength decreased as well. When the welding speed moved too fast, it resulted in the change of immediate heat around the welding tool [11]. These are the reasons for the defected formation of after welding. Moreover, the value of tensile strength could be explained by the changes in microstructure in SZ, good precipitation of Al_2Cu phase (small particles around 4-7 um is the best size and evenly disperse to all around area) was formed, and uniform distribution would have a good effect on the tensile strength as well [12]. On the other hand, sometimes, friction force made Al_2Cu phase broken into large particles lead to lower tensile strength. The tensile strength results of this TWBs with FSW experiment is presented in Fig.6.

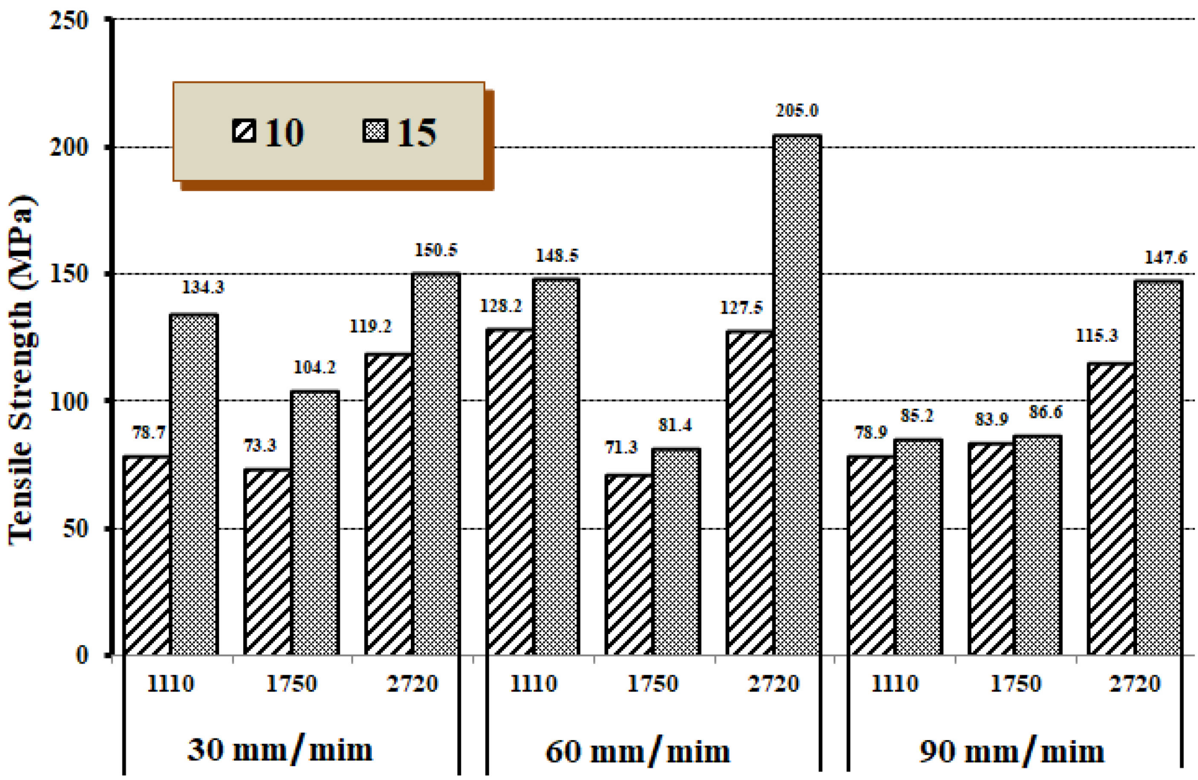

Figure 6. The tensile strength of TWBs with FSW for SSM 2024 aluminium alloy.

Vickers Hardness Results

Figure 7 shows the result of the hardness test of TWBs with FSW for SSM 2024 aluminum alloy. It was found that the SZ had a higher hardness than that of the base metal (BM) caused by the effects of friction force that also caused Al_2Cu phase to be broken and dispersed around the SZ. Moreover, the heat was another cause that affected the structural changes of the SZ until it led to increased hardness [13]. The intermetallic compound was formed by heat, and the transition of the eutectic phase in various forms would promote good hardness. The TMAZ near the SZ showed that the hardness also increased and was influenced by the heat transfer of the welding tool that was radiating during welding. The thermal coefficient of the material affected the width of the TMAZ and widened the area of hardness[14]. However, the BM region received very little heat resulting in the atoms not moving between grains; therefore, the structure was not changed much which would not be able to change the hardness. Another reason was to increase hardness from residual stress derived from material deformation. The friction force caused the SZ to receive stressed during FSW, and some stresses did not release all the energy which still remained inside the material after welding [15]. Likewise, residual stress led to the twisting of the welding samples with a small thickness. In all experiments, the results of hardness were the same direction.

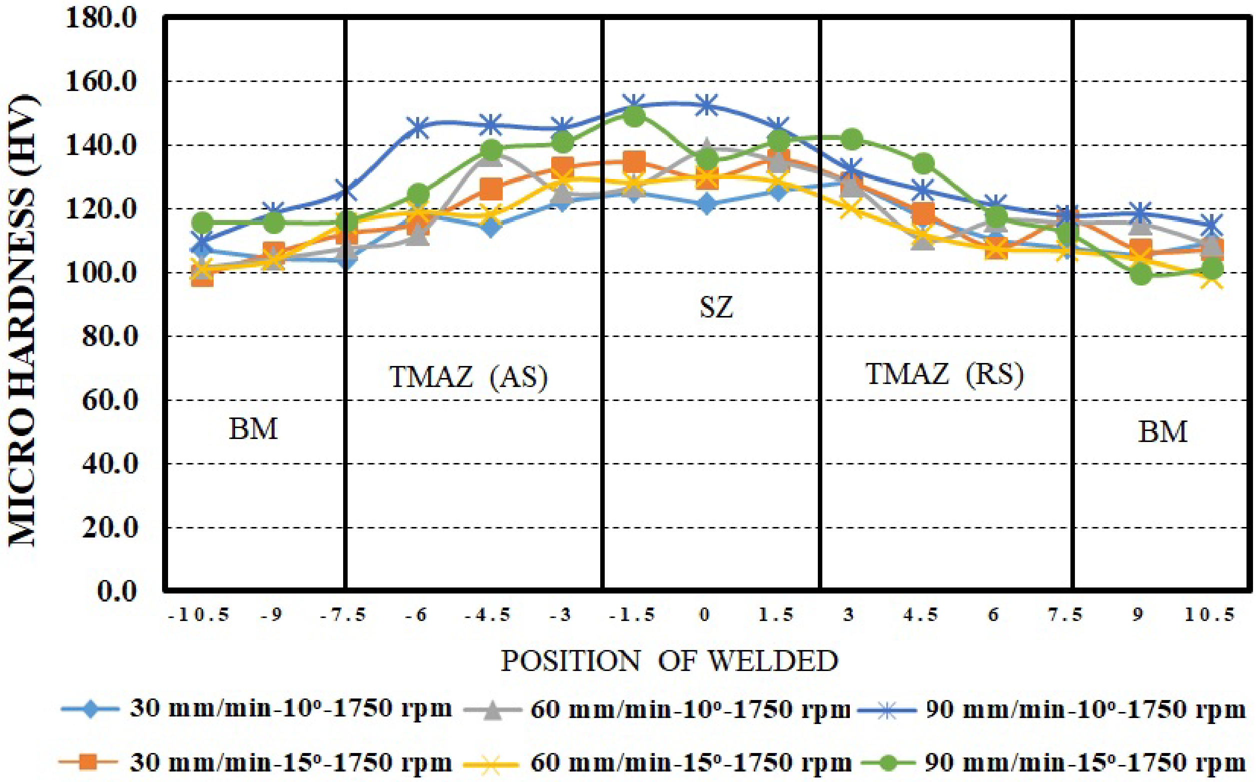

Figures 7. Hardness profiles across the weld region of TWBs with FSW for SSM 2024 aluminium alloy.

Summary

The consideration of suitable variables to the mechanical properties and changes in microstructure is needed for TWBs with FSW for SSM 2024 aluminum alloy. After TWBs to FSW, it was found that variables making Al_2Cu phase into particles with an average size of 4 to 7 µm and distribution throughout the SZ promoted better tensile strength and hardness. The variables at the tilt angle at 15°, rotation speed at 2720 rpm, and welding speed 60 mm/min had a maximum average tensile strength of 205.0 MPa. Meanwhile, the maximum average tensile strength value was 71.3 MPa from tilt angle at 10°, rotation speed at 1750 rpm, and welding speed 60 mm/min respectively. The hardness analysis results showed that SZ had a higher hardness than the TMAZ and BM. This could be explained from the cross-link structure of Al_2Cu phase fracture and plastic deformation in SZ, whilst such structural shape of Al_2Cu phase in TMAZ and BM was less formed, resulting in a low change in hardness. The heat and residual stress were a strong influence on the change of hardness. The higher heat and residual stress during TWBs with FSW for SSM 2024 aluminum alloy with a rotation speed at 2720 rpm, the higher hardness was formed than other variables from the experiment due to the mechanism of generating heat.

Acknowledgment

This work was supported by the Department of Engineering, Faculty of Industrial Technology, and Songkhla Rajabhat University in Thailand.

References

[1] D.M. Rodrigues, B.M. Chaparro, C. Leitao, A.J. Baptista, WELD WORLD. 57 (2007) p. 667-676.

[2] W.M. Thomas and E.D. Nicholas, Mater. Des. 18 (1997) p. 269-273.

[3] R.S. Mishra, Z.Y. Ma, MAT SCI ENG R. 50 (2005) p. 1-78.

[4] Meghnath Sen, Sachindra Shankar, Somnath Chattopadhyaya, Mater. Today. Proc. (2019) p. 1–11.

[5] J. Wannasin and S. Thanabumrungkul, SJST. 30 (2008) p. 215-220.

[6] H.M. Anil Kumar, V. Venakata Ramana, S.P.Shanmuganathan, Mater. Today. Proc. 5 (2018) p. 700–708.

[7] Y.F. Sun, H. Fujii, N. Takaki, Y. Okitsu, Mater. Des. 47 (2013) p. 350–357.

[8] M. Song, R. Kovacevic, Int. J. Mach. 43 (2003) p. 605-615.

[9] W. Xu, J. Liu, G. Luan, and C. Dong, Mater. Des. 30 (2009) p. 1886-1893.

[10] Y.S. Sato, and H. Kokawa, Metall Mater. Trans. A. 32 (2001) p. 3023-3031.

[11] Oluwaseun John Dada, S Afr J. 8 (2020) p. 1-13.

[12] Siva Sitthipong, Prawit Towatana, Chaiyoot Meengam, Suppachai Chainarong and Prapas Muangjunburee, Eng. J. 22 (2018) p. 51-64.

[13] Yongyuth Dunyakul, Chaiyoot Meengam, Dech Maunkhaw and Suhaidee Sani, IJET. 9 (2017) p. 3349-3354.

[14] N. Martinez, N. Kumar, R.S. Mishra, K.J. Doherty, Microstructural variation due to heat gradient of a thick friction stir welded aluminum 7449 alloy, J. Alloys Compd. 713 (2017) 51–56.

[15] Guilherme Vieira Braga Lemos, Alexandre Bellegard Farina, Rafael Menezes Nunes, Pedro Henrique Costa Pereira da Cunha, J MATER RES TECHNOL. 8 (2019) p. 2528-2537.